



HAL
open science

From ICAO GNSS Interference Mask to Jamming Protection Area For Safe Civil Aviation Operation

Guillaume Novella, Christophe Macabiau, Axel Garcia-Pena, Anaïs Martineau, Pierre Ladoux, Philippe Estival, Olivier Troubet-Lacoste, Christian Fleury, Catherine Ronfle-Nadaud

► To cite this version:

Guillaume Novella, Christophe Macabiau, Axel Garcia-Pena, Anaïs Martineau, Pierre Ladoux, et al.. From ICAO GNSS Interference Mask to Jamming Protection Area For Safe Civil Aviation Operation. 34th International Technical Meeting of the Satellite Division of The Institute of Navigation (ION GNSS+ 2021), Sep 2021, St Louis, United States. pp.834-854, 10.33012/2021.17936 . hal-03445703

HAL Id: hal-03445703

<https://enac.hal.science/hal-03445703>

Submitted on 25 Jan 2022

HAL is a multi-disciplinary open access archive for the deposit and dissemination of scientific research documents, whether they are published or not. The documents may come from teaching and research institutions in France or abroad, or from public or private research centers.

L'archive ouverte pluridisciplinaire **HAL**, est destinée au dépôt et à la diffusion de documents scientifiques de niveau recherche, publiés ou non, émanant des établissements d'enseignement et de recherche français ou étrangers, des laboratoires publics ou privés.

From ICAO GNSS Interference Mask to Jamming Protection Area For Safe Civil Aviation Operation

Guillaume Novella, Christophe Macabiau, Axel Garcia-Pena, Anaïs Martineau, *Ecole Nationale de l'Aviation Civile (ENAC)*
Pierre Ladoux, Philippe Estival, Olivier Troubet-Lacoste, Christian Fleury, Catherine Ronfle-Nadaud, *DSNA*

BIOGRAPHIES

Guillaume NOVELLA graduated as a space and aeronautical telecommunications engineer from ENAC (Ecole Nationale de l'Aviation Civile) in 2019. He is now a Ph.D student at the TELECOM lab of the ENAC. His Ph.D topic deals with drone C2Link and GNSS operating margins.

Axel GARCIA-PENA is a researcher/lecturer with the SIGnal processing and NAVigation (SIGNAV) research axis of the TELECOM lab of ENAC (French Civil Aviation University), Toulouse, France. His research interests are GNSS navigation message demodulation, optimization and design, GNSS receiver design and GNSS satellite payload. He received his double engineer degree in 2006 in digital communications from SUPAERO and UPC, and his PhD in 2010 from the Department of Mathematics, Computer Science and Telecommunications of the INPT (Polytechnic National Institute of Toulouse), France.

Christophe MACABIAU graduated as an electronics engineer in 1992 from the ENAC (Ecole Nationale de l'Aviation Civile) in Toulouse, France. Since 1994, he has been working on the application of satellite navigation techniques to civil aviation. He received his Ph.D in 1997 and has been in charge of the signal processing lab of ENAC since 2000, where he also started dealing with navigation techniques for terrestrial navigation. He is currently the head of the TELECOM team of ENAC, that includes research groups on signal processing and navigation, electromagnetics, and data communication networks.

Anaïs Martineau graduated in 2005 as an electronics engineer from the Ecole Nationale de l'Aviation Civile (ENAC) in Toulouse, France. She received her Ph.D. in 2008 from the University of Toulouse. She is now the Head of Electronics, Electromagnetism and Signal Processing Division of the ENAC.

Philippe Estival is a GNSS expert at the French civil aviation service provider (DGAC/DSNA/DTI) currently involved in EGNOS mission requirements and standardization activities on future multi-constellation GNSS receivers Eurocae WG62 and within EU/US cooperation agreement Working Group C. He has been in charge of CCF (EGNOS Central Control Facility) operational support and evolutions for PACF department until 2009 and then for ESSP SAS System Operation Unit up to 2015. He graduated in 2005 as an electronics engineer from French Civil Aviation University, Toulouse, France.

Pierre Ladoux started his career as maintenance engineer on conventional radionavigation aids and then was involved at DSNA/DTI, the French Air Navigation Provider Technical Directorate, in activities related to satellite navigation systems and more specifically on the ICAO standardized Ground Based Augmentation System (GBAS). He is now the head of the Spectrum and Frequency management unit at DSNA.

ABSTRACT

Jamming situations taking place as part of anti-drone struggle or military exercises are a threat for civil aviation. During these jamming operations, in order to protect civil aviation operations, segregation zones (also called protection zone in this article) are elaborated in which GNSS ICAO minimum requirements are not guaranteed. Segregation zones refer to the area, determined by the regulator, in which pilots are warned of a potential GNSS service failure because of the jamming. Currently, these protection areas are deduced from the ITU standardized interference mask but it appears that these protection areas are much larger than the observed impacted zone, highlighting thus the inefficiency of the current method. In this article, first a clarification on the interpretation of the interference mask is proposed, in order to explain the difference between the size of the protection zone and the impacted area. Second, a new method is proposed to compute a new protection zone, and this method estimates the true impacted zone considering

local RFI situation. The main innovation of this new method is to take into account the situation of the jammer in terms of aeronautical interference level in its local surroundings. The main advantage of this method is the protection area size reduction while still guaranteeing that minimum GNSS ICAO requirements are respected.

INTRODUCTION

GNSS signals are vulnerable to Radio Frequency Interferences (RFI) due to their very low power when reaching a GNSS receiver on earth or on an aircraft. RFI can be defined as a transmission of energy that may disturb the behavior of the GNSS receiver. Several RFI classifications can be made, for example distinguishing intentional or unintentional, aeronautical or non-aeronautical RFI. Focusing on civil aviation application, nowadays, an increasing number of RFI sources impact GNSS receivers and threaten aircraft safety.

One of the most important types of RFI affecting civil aviation is intentional (targeted victims) or unintentional jamming (collateral victims), especially state jammers which usage is continuously increasing in order to cope with new safety threats. Indeed, state jamming is expected to become a significant topic of interest since state jamming is used as the main defense tool to counter rogue drones, a rising safety-threatening event and since testing exercises for jammer development continues to grow. To avoid insufficient GNSS performance during state jamming, the ANSP (Air Navigation Service Provider) is in charge of determining the zone where GNSS receivers may not achieve ICAO minimum requirements. In these zones referred as protection zones, pilots are notified of a potential loss of the GNSS link through NOTAM (Notice to Airmen). The reliability in the determination of this zone has a major significance. On the one hand, a too small protection zone will induce safety problems, since the receiver may not be able to meet minimum requirements. On the other hand, a too large protection zone will decrease the flights resources consumption efficiency as explained next. Indeed, pilots would be asked to avoid the protection zone in order to make sure the navigation system meets the performance objectives, resulting in traffic limitations, a larger flight time, larger covered distance and higher fuel consumption.

Currently, the methodology applied by ANSPs to determine the zone impacted by state jamming relies mainly on the use of the ITU standardized RFI mask. The RFI mask provides the maximum power of non-aeronautical RFI that can be tolerated by a receiver to still meet the ICAO performance requirements. However, the ITU standardized RFI mask is derived from a global worst-case or limiting scenario. Indeed, the mask is computed in order to guarantee that GNSS receivers meet ICAO requirements at the world's location where the margin between the required C/N_0 by the different signal processing operation and the link budget C/N_0 obtained in presence of aeronautical RFI sources only yields the smallest tolerable power for all potential non aeronautical RFI sources. As a consequence, the protection area against non-aeronautical RFI which is derived from the RFI mask is an upper bound of any position on Earth which can be too high when only considering the state jammer position local RFI constraints. The aim of this article is thus to provide a method in order to refine the area where GNSS receivers are potentially impacted by the state jamming.

This article is structured in seven sections. First, interference masks are introduced. Second, the traditional method used by ANSP when it comes to derive protection areas is described and its limitations are highlighted. Third, the new method is introduced. Fourth, RFI usually faced by an aeronautical GNSS receiver are analyzed. Fifth, the new method to compute protection zones is detailed. Sixth, a comparison of both methods is done through an illustrative jamming scenario. Finally, the main conclusions of this work are presented.

INTERPRETATION OF THE RFI MASK

The notion of RFI mask is introduced in [1] for L1 and in [2] for L5. The RFI mask provides the maximum power that can be tolerated by an aeronautical receiver at the antenna port to guarantee the fulfillment of $1.\sigma$ performance objective defined by ICAO SARPs [3]. In this section, a focus on the L1 band is proposed. The in-band RFI mask provides the maximum power of a RFI hitting the L1/E1 band ($L1 \pm 10$ MHz) as a function of its bandwidth (double sided). The out-of-band RFI mask gives the maximum power of a 700Hz CW RFI as a function of its central frequency.

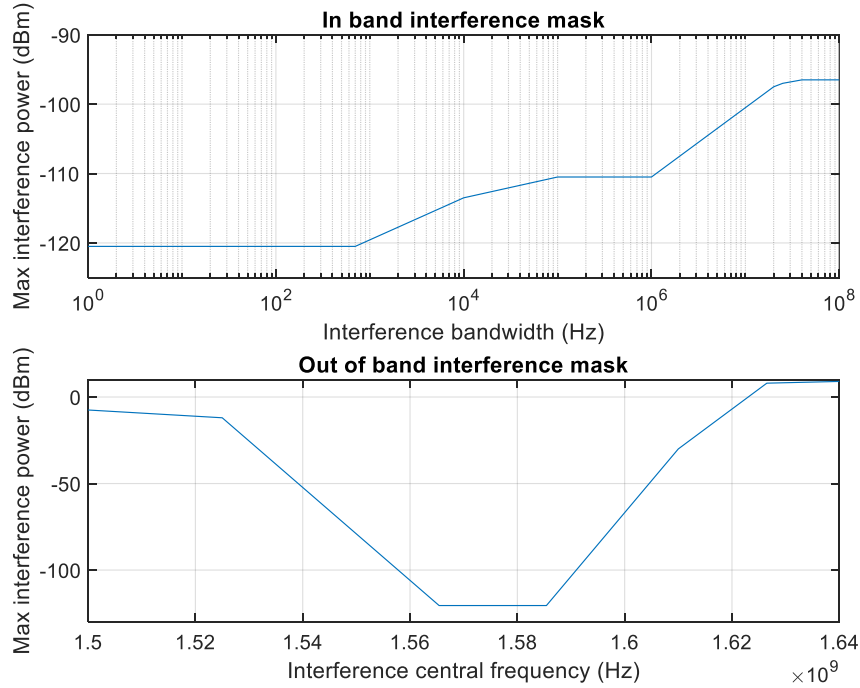


Figure 1: L1 RFI masks

RFI masks represented in Figure 1 are derived for RFI whose power spectral density (PSD) has a rectangular shape. The effect of the RFI on the receiver is attenuated by the correlator. Indeed, the multiplication by the PRN (Pseudo Random Noise) local code spreads the RFI PSD which is then filtered by a narrow-band filter (the integrator block) usually resulting in a significant reduction of the RFI power at the correlator block output with respect to the RFI power at its input. This attenuation of the RFI power is characterized by the processing gain, which is the ratio between the RFI power at the output of the correlator and the power at the input. As highlighted by [4], the processing gain grows with the RFI bandwidth as well as with the frequency offset between the RFI central frequency and the GNSS carrier frequency. The shape of the in-band RFI mask is thus linked with the variation of the processing gain. Moreover, when the RFI central frequency is outside the GNSS band, in addition to the processing gain brought by the correlation, the antenna frequency rejection as well as the RF front-end filter help in attenuating the RFI. The aggregate attenuation (total attenuation of the RFI brought by the processing gain, the antenna rejection and the RF/IF filter rejection) in the out-of-band part of the spectrum gives the shape of the out-of-band RFI mask.

ANSP TRADITIONAL METHOD FOR PROTECTIONZONE COMPUTATION

RFI mask is the tool which is usually used to derive protection zones during state jamming exercises. Indeed, ANSP traditional method allocates to the jammer signal all the non-aeronautical power at the antenna port provided by the RFI mask. Therefore, the protection zone computed from the RFI mask method when only considering free space losses is a half sphere whose radius is

$$r(G_J, G_{rcv}) = \frac{\lambda}{4 \cdot \pi} \cdot \sqrt{\frac{P_J \cdot G_J \cdot G_{rcv}}{C_{max}}} \quad (1)$$

λ is the jammer signal wavelength, P_J is the jamming signal power, G_J is the jammer antenna gain, G_{rcv} is the receiver antenna gain in the direction of the jammer and C_{max} is the maximum non-aeronautical RFI power given by the RFI mask. Usually, it is assumed that the jammer transmission direction is unknown. Therefore, to compute the protection zone radius, the maximum values of the transmitter and receiver antenna gain patterns are used in equation (1), $r_{max} = r(G_{J,max}, G_{rcv,max})$.

The use of the RFI mask as the basic input parameter is not always adapted to the elaboration of protection zones for several reasons. First of all, RFI masks aim to assess the worst situation of GNSS receivers in presence of aeronautical and non-aeronautical RFI in

any point on Earth. Thus, RFI masks reflect a situation where aeronautical RFI are strong (equal or close to its highest power value). For the L1 band in particular, the RFI mask reflects the maximum tolerable power that can be tolerated in Honolulu during precision approach. As a consequence, the aeronautical RFI environment in the vicinity of the jammer may not correspond to the situation from which the RFI mask is derived (Honolulu). Second, RFI masks are not adapted to all types of RFI. Indeed, RFI masks represented in Figure 1 are derived for RFI whose power spectral density has a rectangular shape. As a result, RFI masks do not guarantee the fulfillment of minimum GNSS requirements if the RFI has a different power spectral density shape, since the processing gain should also be different. Finally, the RFI masks provide the total non-aeronautical RFI power. This non-aeronautical power must be shared between several non-aeronautical sources which are already present on the surroundings of the state jammer. Thus, all the non-aeronautical level read on the RFI mask cannot be allocated to the jamming signal.

INTRODUCTION TO A NEW METHOD FOR PROTECTION AREA COMPUTATION

The new proposed method to elaborate protection zones during jamming exercises is expected to remove disadvantages of the traditional method based on the RFI mask. In most locations in the world, the aeronautical RFI has a weaker power in comparison to aeronautical RFI environment associated to the RFI mask. Therefore, in these locations, the GNSS receiver should be able to tolerate more non-aeronautical RFI power than the power indicated by the RFI mask. Indeed, the GNSS RFI mask is derived such that the aggregate RFI level (aeronautical RFI plus non-aeronautical RFI) is the RFI level that can be tolerated by the receiver, keeping minimum ICAO operational requirements fulfilled. As a consequence, if aeronautical RFI power is lower than the aeronautical RFI power considered when elaborating the RFI mask, then the receiver should be able to operate even though the non-aeronautical RFI level is above the RFI mask, provided that the total RFI level remains lower than the maximum aggregate RFI power tolerated by the receiver to meet minimum ICAO operational requirements.

The fundamental idea of this new method consists thus in allocating the extra margin, left by a favorable aeronautical situation in comparison to the RFI situation associated with the RFI mask, to non-aeronautical RFI. In addition, the RFI mask has been elaborated to protect legacy GNSS receivers from non-aeronautical RFI. Dual Frequency Multi Constellation (DFMC) receivers are more robust facing RFI than legacy receiver, thanks to lower implementation losses and a better antenna gain [5]. This article will focus on DFMC receivers which inherently bring some capability to tolerate more non-aeronautical RFI. Moreover, note that ITU standardized RFI mask will not tolerate more RFI power with the introduction of DFMC receivers since the RFI mask has still to protect legacy receivers.

In conclusion, since the GNSS receiver can tolerate more non-aeronautical RFI power than the power indicated by the RFI mask, due to a potential decrease of aeronautical RFI power and due to the use of DFMC receivers, then minimum operational requirements can be met even though the victim receiver is inside the protection zone determined by the traditional method.

One important remark to consider about the new proposed method is the following one. During their certification phase, the GNSS receiver resiliency to RFI is tested by injecting non-aeronautical RFI, whose power is determined by the RFI mask, and by injecting aeronautical RFI, which power is chosen as a function of the receiver's test location. This means that if this new method for the determination of the protection area is used, the receiver should be able to tolerate a higher level of non-aeronautical RFI than the one used for receiver testing. However, the total RFI level (aeronautical and non-aeronautical) to which the receiver is tested remains unchanged.

LIST OF AERONAUTICAL RFI SOURCES

This article focuses on the L1 band in particular. Indeed, most of the jamming exercises that currently take place target the L1 band. However, the methodology proposed in this article can also be applied to the L5 band. The main difference will be the list of aeronautical RFI sources impacting the GNSS band, in particular, pulsed aeronautical RFI from DME, TACAN, JTIDS/MIDS. The impact of these RFI sources hitting the L5 band has been listed in [2] and studied in [6].

[7] identifies three aeronautical RFI sources transmitting in or in the vicinity of the GNSS L1 band (1559-1610 MHz):

- 1) AMSS: Some aircrafts have an aeronautical mobile satellite system (AMSS) equipment. This on-board equipment allows communication between the crew and the ground through satellite communications. AMSS has a frequency allocation in the [1626-1660] MHz band and thus, AMSS transmission does not directly hit the GNSS L1 band. However, 5th and 7th order intermodulations fall into the L1 GNSS band and may degrade GNSS signal processing.
- 2) Case Emission: Cockpit devices screens also radiate unwanted energy in the GNSS L1 band. This aeronautical RFI source is referred as case emission. Current cockpit installed equipment are tested and certified according to [8] Cat M requirements. In particular, undesired radiation in the GNSS frequency band from each cockpit equipment device is limited

to 53.3 dB μ V/m for this category of equipment. Newer cockpit devices will be certified according to Cat P and Cat Q requirements and will be allowed to transmit no more than 40 dB μ V/m.

- 3) Inter and intra system RFI: Inter and intra system RFI refers to GNSS signals coming from other GNSS constellations or from the same constellation but different from the signal of interest. For example, Galileo E1 signals and GPS L1C/A PRN 6 signal act as an RFI on the receiver channel processing GPS L1C/A PRN 2 signal. Since there are more and more GNSS constellations, inter system RFI should be regularly revised. In particular, the RFI mask is based on an inter/intra system RFI analysis performed in 2004, which do not consider Beidou signals. Thus, aeronautical RFI computation is not up to date in the RFI mask.

IMPACT OF RFI SOURCES ON GNSS RECEIVER

RFI sources impact on GNSS receiver is modelled as an increase of the noise floor at the GNSS antenna port (although this modelling is not accurate for RFI with bandwidth smaller than the inverse of the correlation integration time). Indeed, signals using code division multiple access (CDMA) spread spectrum techniques are based on the spreading of a useful signal thanks to the multiplication with the pseudo random noise (PRN) code. In the receiver, the received signal is multiplied by a locally generated PRN code. The goal of this operation is to remove the PRN code on the useful signal in order to de-spread the useful signal. Other components of the received signal such as RFI are meanwhile spread by the multiplication with the locally generated PRN code and are modelled as an AWGN. More details on the behavior of RFI on CDMA receivers can be found in [4].

The equivalent noise of an RFI source X is defined by the power spectral density $I_{0,X}$ of an AWGN that would result in the same power at the correlator output than the RFI. The equivalent noise $I_{0,X}$ of an RFI source is calculated by the multiplication of the RFI power at the correlator input C_X with the spectral separation coefficient SSC . The spectral separation coefficient characterizes the correlation between the RFI at the Radio-Frequency Front-End (RFFE) output and the GNSS local replica. It is defined by:

$$SSC = \int_{-\infty}^{+\infty} |H_{RF,BB}(f)|^2 \cdot S_{I,BB}(f) \cdot (S_{cm}(f) * |H_{ID}(f)|^2) \cdot df \quad (2)$$

$H_{RF,BB}$ is the equivalent baseband transfer function of the RFFE. $S_{I,BB}$ is the equivalent baseband normalized (unit power) power spectral density of the RFI signal. S_{cm} is the power spectral density of the PRN modulated signal. H_{ID} is the power spectral density of the integrate and dump filter. H_{ID} can also be expressed as $H_{ID} = \sqrt{T_I} \cdot \text{sinc}(\pi \cdot f \cdot T_I)$, where T_I is the correlation integration duration.

[7] and [9] compute the equivalent noise caused by the different aeronautical sources impacting the L1 band. The main steps of this computation are recalled hereinafter.

1. AMSS: AMSS services transmit in the sub-bands [1545-1559] MHz and [1646.5-1660.5] MHz. Even though a selection on transmitting AMSS channels is done in order to avoid that high order inter modulation products fall close to L1, the L1/E1 band may be affected by the fifth and seventh order inter modulation product with a power up to -159 dBW (measured in a 1 MHz bandwidth). Assuming that the bandwidth of the AMSS inter-modulation is large enough to be considered as AWGN, each AMSS terminal creates an equivalent noise equal to -159 dBW/MHz. It is considered that two AMSS terminal in idle mode (each creating an equivalent noise equal to -162 dBW/MHz) and one AMSS terminal operating creates RFI on the GNSS L1 band. As a consequence, the total equivalent noise induced by AMSS is

$$I_{0,AMSS} = -155.98 \text{ dBW/MHz} \quad (3)$$

2. Case Emission: First, even though Cat M cockpit equipment are allowed to radiate up to 53.3 dB μ V/m in the L1/E1 band, measurements performed by [7] show that the cockpit devices transmit at a lower level in this frequency band. Therefore, it is proposed to bound the electric field transmitted in the L1 band by one cockpit equipment by 40 dB μ V/m, measured on a 1 MHz bandwidth [7]. Moreover, newer generation Cat P and Cat Q equipment are not allowed to radiate more than 40 dB μ V/m in the L1/E1 band. Second, the path loss (PL) between the cockpit window and the GNSS antenna is measured by [10] at PL=65 dB. Third and last, 10 devices are assumed to be installed in the cockpit. In addition, 2 additional devices are considered, corresponding to electronic flight bags (EFB) often carried by pilots. Although EFB are not restricted by DO160,

measurement shows that their radiation in the L1 band is lower than $E=40 \text{ dB}\mu\text{V/m}$. Case emission RFI is also supposed to be AWGN. Therefore, the equivalent noise caused by case emission RFI source is [7]

$$I_{0,case\ em} = \frac{E^2}{30} \cdot N \cdot PL = -148.98 \text{ dBW/MHz} \quad (4)$$

$N = 12$ is the number of cockpit devices interfering with the GNSS signal.

3. **Inter and intra system RFI:** Inter and intra system RFI depends on the constellations configuration at the time of the state jamming operation. However, in this work, in order to cover for a worst situation and in order to reduce the method's calculation time, it is proposed to provide an upper bound of the equivalent noise caused by inter/intra system RFI: to provide the highest value among all time epochs at each location in the world. As a result, values provided in this article can be re-used for future jamming exercise.

The approach using spectral separation coefficient is adopted. A GNSS signal j creates an equivalent noise on the channel processing a different GNSS i signal at a given time t epoch and at a given location \mathbf{x} equal to

$$I_{0,j}(t, \mathbf{x}) = C_j(t, \mathbf{x}) \cdot SSC_{i,j} \quad (5)$$

Where C_j is the equivalent recovered signal power j at the antenna port assuming that the RFFE block and the correlator block are ideal (no additional power losses are introduced by these elements) and $SSC_{i,j}$ is the spectral separation coefficient between signals i and j .

On the one hand, C_j is the product between the GNSS RFI received power on Earth P_{max} (specified in interface control document), the aggregate GNSS antenna gain G_{mean} (transmitter plus receiver antenna gain) and some losses $L_{imp,gnss}$.

$$C_j(t, \mathbf{x}) = P_{max} \cdot G_{mean}(t, \mathbf{x}) \cdot L_{imp,gnss} \quad (6)$$

Table 1 provides the characteristics of each GNSS signal in the L1/E1 band that are considered in this article.

System	Signal	Modulation	Central Frequency (MHz)	Orbit	Number of sats to consider	Localisation for GEOs	Tx BW (MHz)	Min Power (dBW)	Max Power (dBW)
BEIDOU	B1-C data	BOC(1,1)	1575,42	MEO+ IGSO+ GEO	27+3+5	58.75, 80, 110.5, 140, 160	40,92	-163	-156
	B1-C pilot	QMBOC(6,1,4/33)	1575,42					-158,25	-151,25
	SBAS	bPSK(1)	1575.42					-158,5	-152,5
	E2I	BPSK(2)	1561.098					-163	-160
	E2Q	BPSK(2)	1561.098					-157	-150
Galileo	E1-F data	CBOC(6,1,1/11,'+')	1575,42	MEO	30 considered		40,92	-160	-153
	E1-F pilot	CBOC(6,1,1/11,'-')	1575,42					-160	-153
	E1-P	BOCc(15,2.5)	1575,42					-157	-150
GPS	L1 C/A	BPSK(1)	1575,42	MEO	30 considered		30,69	-158,5	-153

	L1C - data	BOC(1,1)	1575,42					-163	-156
	L1C - pilot	TMBOC(6,1,4/33)	1575,42					-158,25	-151,25
	P(Y)	BPSK(10)	1575,42					-161,5	-150
	M-Code	BOC(10,5)	1575,42					-157	-150
QZSS	L1 C/A	BPSK(1)	1575,42	HEO+ GEO	3 IGSO + 4 GEO		24	-158,5	-153
	L1C data	BOC(1,1)	1575,42					-163	-160
	L1C pilot	TMBOC(6,1,4/33)	1575,42					-158,25	-155,25
	SBAS	BPSK(1)						-158,5	-152,5
	L1 SAIF	BPSK(1)	1575,42					-161	-153
EGNOS	SBAS	BPSK(1)	1575,42	GEO	3	-15.5, 5, 31.5	4	-161	-152,5
WAAS	SBAS	BPSK(1)	1575,42	GEO	3	-98 -117 -129	24	-158,5	-152,5
GAGAN	SBAS	BPSK(1)	1575,42	GEO	2 + 1 spare	55, 83, 93.5	24	-158,5	-152,5
SDCM	SBAS	BPSK(1)	1575,42	GEO	3	167, 95, 16	24	-158,5	-152,5
KASS	SBAS	BPSK(1)	1575,42	GEO	2	125, 130	24	-158,5	-152,5
African SBAS	SBAS	BPSK(1)	1575,42	GEO	3	-20, 15, 55	24	-158,5	-152,5

Table 1: Characteristics of GNSS signals in the L1 band

First, the received signal power depends on satellite transmission power, transmission antenna gain pattern, atmosphere, ionosphere and troposphere attenuation. In this analysis, the satellite transmission power is set to its maximum value that can be read in Table 1. The emitter antenna gain, and the propagation attenuation are taken into account according to Figure 2 as a function of the elevation, for the difference core constellation (GPS, Galileo, Beidou) and satellite based augmentation systems transmitting in the L1/E1 band. The patterns shown in Figure 2 is consistent with the ones used for the inter and intra system RFI analysis performed in [9].

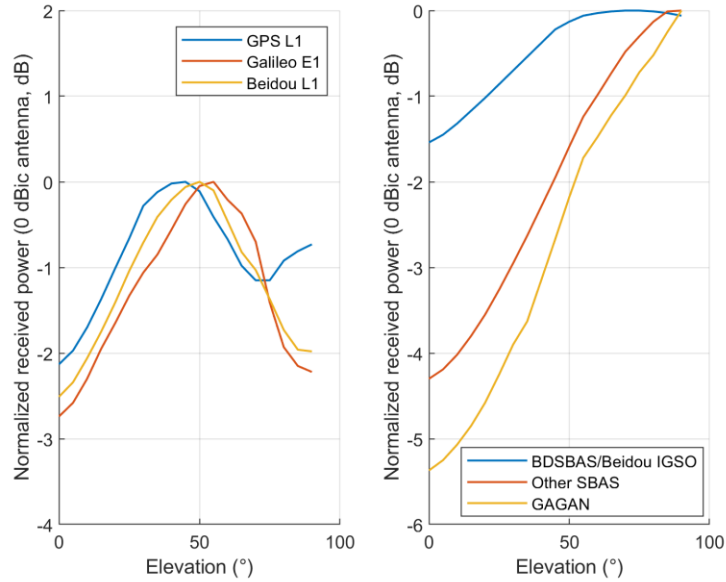


Figure 2: Transmit antenna gain and propagation attenuation pattern

[11] provides requirements on the minimum and the maximum antenna gain of GNSS receiver. Instead of using the maximum antenna gain for all GNSS RFI signals for inter/intra system RFI computation that would represent a very pessimistic case, it is proposed to adopt a “mean” receiver antenna gain pattern. This “mean” receiver antenna gain pattern is shown in Figure 3 and is similar to the antenna gain used in [7] to compute the inter/intra system RFI equivalent noise.

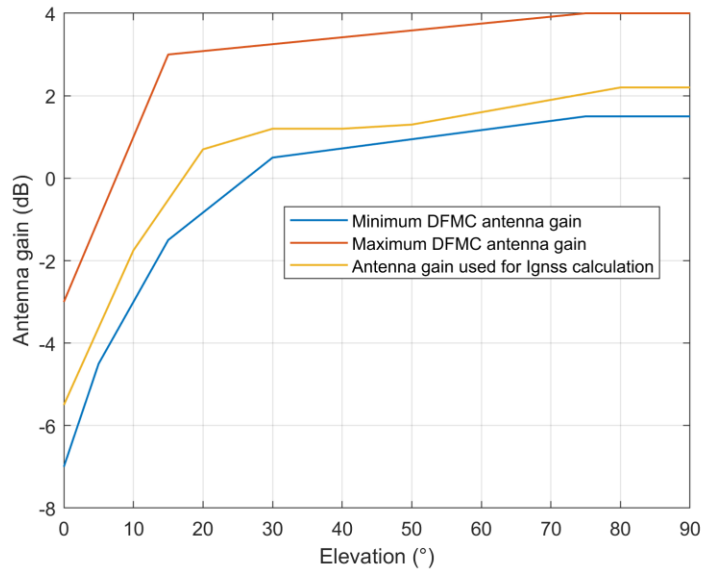


Figure 3: Minimum, maximum DFMC antenna gains and the “mean” antenna gain used for intra and inter system RFI calculation

In equation (6), the antenna gain term $G_{mean}(t, \mathbf{x})$ depends on the time as well as the position of the victim receiver. Indeed, the inter and intra system RFI level depends on the configuration of the GNSS constellation, in particular on the elevation of the different satellites visible by the receiver. Therefore, the inter and intra system RFI equivalent noise is linked with the position of the victim receiver and with the time.

Finally, some losses $L_{imp,gnss}$ must be considered because of payload distortion and quantization. The filtering and correlation impacts are already taken into account when computing the spectral separation coefficient. A 1.516 dB losses is added, in order to take into account the loss of GNSS signal power losses due to 1.5 bit quantization (minimum losses of 0.916 dB, [12]) and to payload distortion (0.6 dB, [13] and [14]).

On the other hand, spectral separation coefficients must be computed as presented in equation (5). Standardized airborne GNSS receivers will use a BOC(1;1) modulated local replica for the synchronization of the Galileo received signals whereas for GPS signals, a BPSK(1) modulated local replica is implemented. Chip modulations of the interfering GNSS signals are recapped in Table 1. Results of the spectral separation coefficient computation for the different modulation of interfering signal are presented in Table 2. A 12 MHz double sided receiver is considered.

System	GNSS signal	Modulation	SSC with BOC(1;1) Galileo E1 receiver in dB	SSC with BPSK(1) GPS L1C/A receiver in dB
Beidou	B1C data	CBOC(6,1,1/11,+)	-65.02	-67.87
	B1C pilot	CBOC(6,1,1/11,-)	-65.35	-68.53
	E2I	BPSK(2)	-91.21	-95.94
	E2Q	BPSK(2)	-91.21	-95.94
Galileo	E1 data	CBOC(6,1,1/11,+)	-65.02	-67.87
	E1 pilot	CBOC(6,1,1/11,-)	-65.35	-68.53
	E1A	BOCc(15,2,5)	-110.92	-115.10
GPS	L1 C/A	BPSK(1)	-67.85	-61.83
	L1C data	BOC(1,1)	-64.78	-67.79
	L1C pilot	TMBOC(6,1,4/33)	-65.25	-68.25
	P(Y)	BPSK(10)	-70.26	-69.94
	M	BOC(10,5)	-83.77	-88.53
QZSS	L1C data	BOC(1,1)	-64.76	-67.77
	L1C pilot	TMBOC(6,1,4/33)	-65.23	-68.23
	C/A, SAIF	BPSK(1)	-67.84	-61.82
SBAS	Beidou, EGNOS, WAAS, GAGAN, MSAS, SDCM, ASECNA	BPSK(1)	-67.84	-61.82

Table 2: Spectral separation coefficient for several GNSS interfering signals (12 MHz double sided receiver)

Note that a different approach is adopted in [5] to compute inter and intra system RFI level on a GPS L1C/A receiver. That approach in [5] aims to take into account alignment of GNSS signal spectrum of BPSK chip modulated GNSS signals (GPS L1C/A, QZSS L1C/A, SBAS). For simplicity purpose and because result differences are small in Europe, the method presented here and the result presented hereinafter are consistent with the inter-intra system computation method developed in [7].

To compute the worst-case total inter/intra system RFI equivalent noise on any location on Earth $I_{0,GNSS}(\mathbf{x}) = \max_t \sum_j C_j(t, \mathbf{x}) \cdot SSC_{i,j}$, constellations are run over one sidereal day to obtain the position of the satellites. From the satellite positions at a given instant t and the known position of the victim receiver, the elevation angle is computed. The elevation angle allows to compute the aggregate GNSS antenna gain (emitter and receiver, see Figure 2 and Figure 3) and then the recovered RFI signal power C_j . The total inter/intra system RFI equivalent noise will be the sum of contributions of all GNSS interfering signals visible by the victim receiver. GNSS constellations are treated differently with respect to regional systems and SBAS:

- GNSS constellations: It is assumed that a global constellation will drift over time in the East-West direction with respect to the Earth axis, and that different core constellations will drift with respect to each other. This means that the worst I_{GNSS} created by a given core constellation will be provided only as a function of the latitude, and that the contribution of each constellation can be calculated independently from the others. The worst case aggregate I_{GNSS} per latitude from all global constellations will thus be the sum of the worst contribution of each individual constellation per latitude.
- Regional and SBAS systems: they are meant to provide a service in a specific well-defined area and thus, it is considered that the associated constellation does not drift in the East-West direction over time with respect to the Earth axis. In this case, the worst contribution of the SBAS and regional systems to the total I_{GNSS} is computed for each point of a world grid.

Note that the different processing of the 2 above categories (global versus regional systems) means that some systems, such as BeiDou are split between their global and regional parts in the I_{GNSS} computation. Figure 4 and Figure 5 show the worst-case aggregate inter and intra system RFI equivalent noise for a Galileo E1 and GPS L1C/A receiver, considering assumptions presented above.

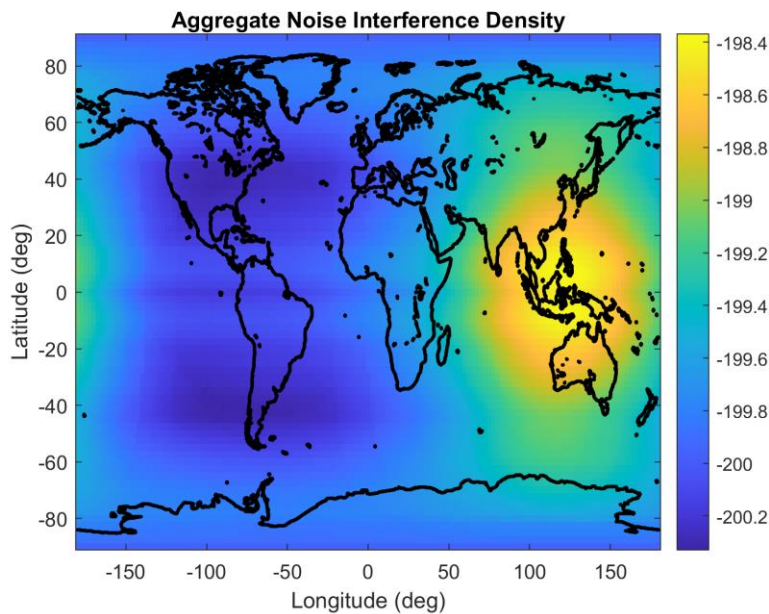


Figure 4: Worst case aggregate inter and intra system RFI equivalent noise on a BOC(1,1) Galileo E1 receiver

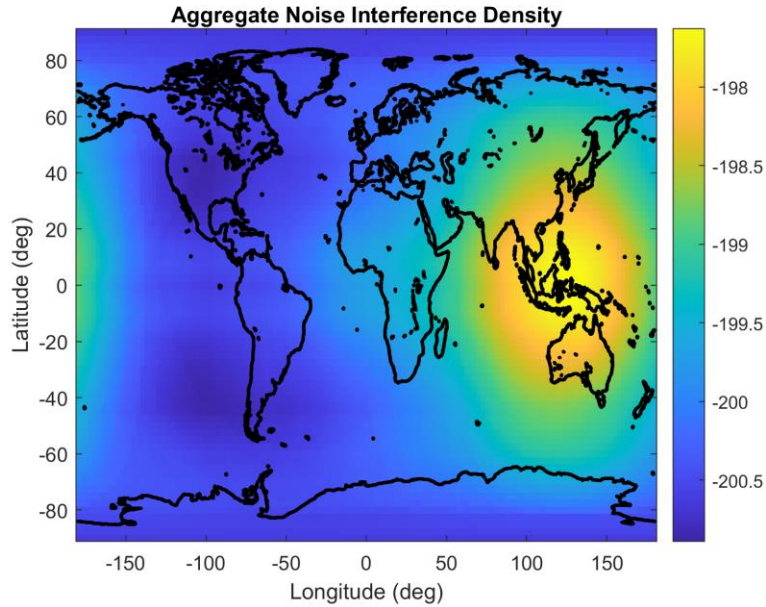


Figure 5: Worst case aggregate inter and intra system RFI equivalent noise on a BPSK(1) GPS L1C/A receiver

Figure 4 and Figure 5 highlights a huge dependence between the receiver position and the inter and intra system RFI equivalent noise. Inter/intra system RFI level is high in south east Asia because of a huge concentration of regional constellation. Conversely, at the point where the jamming of the illustrative situation occurs, the aeronautical RFI level is around 2 dB lower. Remember that the fundamental idea of the proposed methodology to derive protection zone is to allocate the room left by a lower aeronautical RFI level to non-aeronautical RFI.

NON-AERONAUTICAL RFI SOURCES

The maximum tolerable non-aeronautical equivalent noise must be shared between different non-aeronautical RFI sources that impact the L1 band. Three non-aeronautical RFI sources impacting the L1 band are identified. First, portable electronic devices (PEDs) carried by passengers on-board of the airplane radiate unwanted energy in the L1 band. Second, the GNSS antenna receive undesired energy from ground emitters of various type (PEDs, cellular antenna, Wifi) [13]. Finally, the jammer is also part of the non-aeronautical RFI sources.

On-board PEDs: Passengers are allowed to use their electronic devices during some phases of the flight. These electronic devices carried by passengers are referred to as on-board portable electronic devices. NASA performed measurements on several kinds of PEDs (laptop, mobile phones, etc) [10] [15]. The equivalent noise caused by on-board PEDs is calculated as:

$$I_{0,on\ board} = \sum EIRP \cdot PL \quad (7)$$

The mean EIRP transmitted by a single device is estimated at -75.2 dBm in [7]. Taking into account the correction due to the antenna used by NASA during their measurement, and supposing that the PEDs transmission is broadband, the equivalent noise transmitted by a single on-board PED is estimated to -96.2 dBW/Hz. [10] also performed measurement on the path loss (PL) between all seats inside a Boeing 737-200 aircraft and the GNSS antenna. Path losses varies between 64.2 dB and 90.1 dB for seats located close to a window. Considering that all passengers are simultaneously using an electronic device, the on-board PEDs equivalent noise becomes -208.9 dBW/Hz. However, the hypothesis considering that all passengers are simultaneously using an electronic device seems quite conservative. Instead, [7] considers that half of the front half seats and 25% of rear half seats near windows are using a PED. Considering this hypothesis, the equivalent noise transmitted by PEDs carried by passengers reduces to $I_{0,on\ board} = -212.5$ dBW/Hz. This calculation holds some uncertainties: power transmitted by each individual PED, number of passengers carrying PED, path losses between the cabin and the GNSS antenna for example. Thus, a 6 dB margin is added on equivalent noise caused by on-board PEDs to cover all potential power fluctuation from the mean power as well as the listed uncertainties.

Terrestrial emitters: Terrestrial emitters refer to a wide variety of devices unvoluntary radiating in the GNSS band with low power: PEDs, wifi sources, etc. The terrestrial emitter RFI level received by a victim GNSS antenna depends on the environment. Indeed, the density of emitters is much higher when the airplane is above an urban area than when the airplane is flying above the sea. It is here proposed to consider a density of emitters equal to $10^{-4} \cdot \text{m}^{-2}$ in urban areas; a density of $0.33 \cdot 10^{-4} \cdot \text{m}^{-2}$ in other terrestrial zones and no emission coming from desertic zones (ocean for example). These density values are recommended in [7]. Moreover, the altitude of the aircraft also influences the impact of terrestrial emitters on the receiver. On the one hand, the number of emitters visible from the on-board antenna grows with the altitude of the aircraft. On the other hand, attenuation due to propagation losses also grows with the aircraft altitude. The equivalent noise caused by terrestrial emitters is thus obtained integrating the radiated emission from each elementary area visible from the aircraft antenna.

$$I_{0,\text{terr}} = \int_0^{R_{\text{LOS}}} \int_0^{2\pi} P_0 \cdot d(r, \varphi) \cdot G_{\text{rcv}}(\varphi) \cdot \left(\frac{\lambda}{4 \cdot \pi \cdot r}\right)^2 r \cdot d\varphi \cdot dr \quad (8)$$

Where P_0 is the radiated power in the L1 band by a single device, R_{LOS} is the electrical radio horizon, d is the density of emitters of the elementary area, G_{rcv} is the lower hemisphere maximum antenna gain. P_0 is chosen to be equal to -81.1 dBW/MHz in [9] Appendix I. This choice is driven by an analysis conducted by NASA [15]. G_{rcv} is represented in Figure 6 for a DFMC antenna and respects [11] specifications

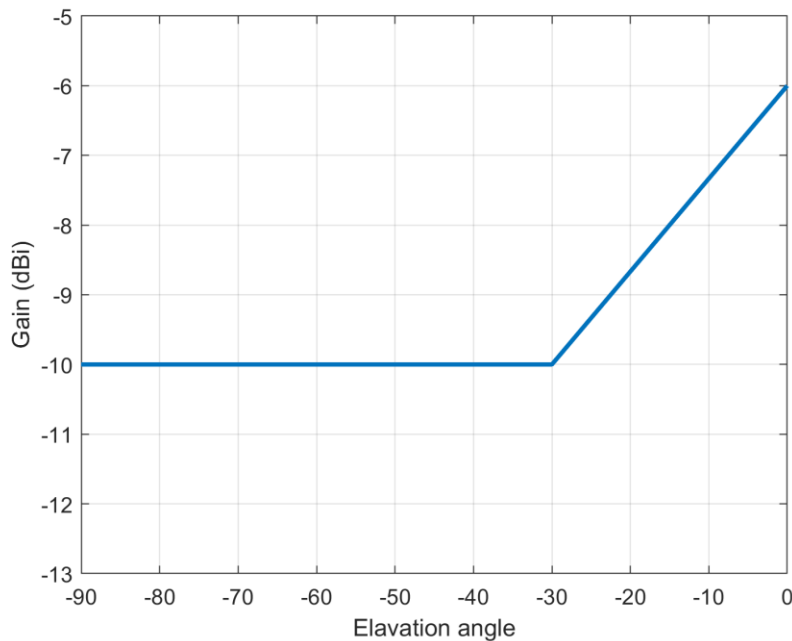


Figure 6: Maximum DFMC lower hemisphere antenna gain

A conservative free space losses propagation model is adopted in equation (8). More developed models can be also proposed in order to refine the result; for example, Hata Okumura model allows to characterize the environment. Finally, Figure 7 shows the equivalent noise caused by terrestrial emitters and received by an aircraft with a 500 m altitude around the jammer position. The blue point represents the jammer position. It is proposed to add a 6 dB margin to the result because of potential power fluctuation from the mean power as well as uncertainties on the calculation of the equivalent noise caused by terrestrial emitters.

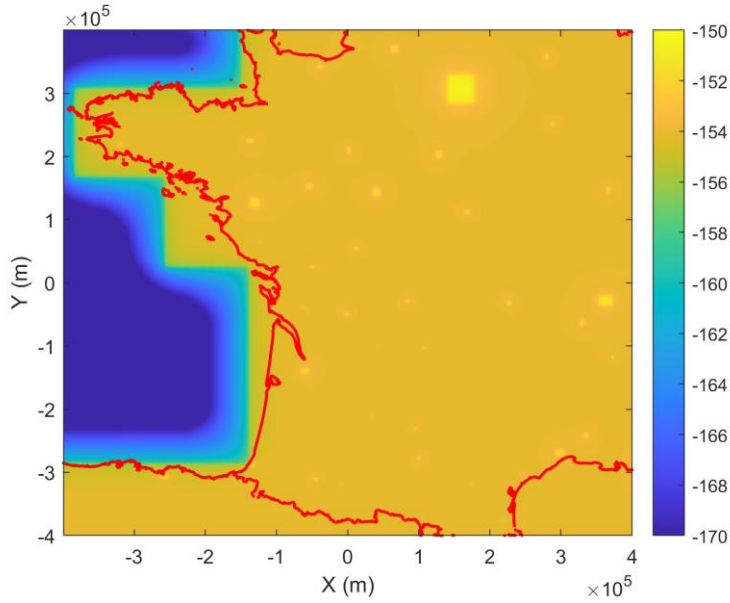


Figure 7: Equivalent noise (dBW/MHz) caused by terrestrial emitters at a 500 m altitude

Figure 7 highlights the link between the area below the victim aircraft and the non-aeronautical RFI level. As expected, the equivalent noise caused by terrestrial emitters is high above urban areas (since the density of emitters is high, with a low propagation loss) and low above ocean zones. Above rural areas, the non-aeronautical RFI level varies between -152 and -154 dBW/MHz. The map is centered on the position 46.1°N, 0.18°E.

Jammer: The effect of the jammer signal on the receiver is, as for all RFI, characterized by the increase of the noise at the antenna port. This increase can be modelled using the SSC formula (equation (2)) if the jammer PSD shape is known. The equivalent noise output induced by the jammer is given by

$$I_{0,jam} = C_j \cdot SSC_j \quad (9)$$

C_j is the power of the jamming signal at the antenna port. SSC_j is the spectral separation coefficient between the jamming signal and the locally generated GNSS signal. In order to be conservative, and since the impact of ADC on jamming RFI power is not precisely known, no implementation losses is added on the jamming RFI power. A free space loss propagation model is adopted in this article. As a result, the power of the jamming signal at the antenna port is given by:

$$C_j(\varphi) = P_j \cdot G_j \cdot G_{rcv}(\varphi) \cdot \left(\frac{\lambda}{4 \cdot \pi \cdot r} \right)^2 \quad (10)$$

P_j is the power of the jammer transmitter, G_j is the antenna gain of the transmitter antenna in the direction of the aircraft. G_{rcv} is the receiver antenna gain, $G_{rcv}(\varphi)$ depends on the elevation angle of the jammer with respect to the aircraft. λ is the jamming signal wavelength and r is the distance between the jammer and the victim antenna. If the jammer is very powerful, the free space loss propagation model is too conservative, since reflection of the jamming signal on the troposphere also makes the noise level at the antenna port increase.

DETAIL OF THE NEW METHOD TO COMPUTE PROTECTIONS AREAS

This section mathematically describes the new proposed method. The objective of the method is to identify all victim receiver positions for which minimum ICAO operation requirements are not respected because of the jammer impact. At least all victim receiver locations which are in Radio Line of Sight (RLOS) from the jammer will be investigated. For other positions for which the jammer is not visible, the jammer cannot cause a disruption of the GNSS service and thus they do not need to be investigated. This method is divided in three steps:

1. Computation of the maximum non-aeronautical RFI tolerated by the receiver.
 - 1.1 Computation the recovered useful GNSS signal power at the antenna port (inputs: receiver position and jamming date)
 - 1.2 Computation of the effective noise in presence of aeronautical RFI.
 - 1.3 Deduction of the link budget margin.
 - 1.4 Computation of the maximum non-aeronautical RFI tolerated by the receiver
2. Computation of the non-aeronautical equivalent noise
3. Deduction of the protection zone

1. Computation of maximum tolerable non-aeronautical RFI level:

First, the maximum tolerable non-aeronautical RFI level is computed at victim receiver positions in RLOS from the jammer. In order to achieve this step, four intermediate computations are done. First, the minimum recovered GNSS signal power is computed. Second, the effective noise $N_{0,eff,only,aero}$ in presence of aeronautical RFI is computed. Third, the C/N_0 link budget margin is computed. Finally, the maximum tolerable non-aeronautical equivalent noise is deduced.

Minimum ICAO requirements on acquisition, tracking and demodulation are translated into a carrier to noise density ratio objectives. A C/N_0 link budget analysis compares the minimum C/N_0 in presence of aeronautical RFI only in the vicinity of the receiver, $C/N_{0,eff,only,aero}$, with the C/N_0 threshold for the considered operation (acquisition, tracking, demodulation), $C/N_{0,th}$. The maximum tolerable non-aeronautical RFI level is defined by the RFI equivalent noise that can be added in the link budget to decrease the original $C/N_{0,eff,only,aero}$ down to the $C/N_{0,th}$. $C/N_{0,th}$ depends on the operation (acquisition, tracking, demodulation) and on the processed signal. Table 3 provides $C/N_{0,th}$ for the different GNSS operations and signals processed by a DMFC receiver.

Signal	GPS L1C/A			SBAS L1	Galileo E1OS		
	First SV acquisition	2 nd – 4 th SV acquisition	Tracking	Demodulation	First SV acquisition	2 nd – 4 th SV acquisition	Tracking
C/N0 threshold	32.4	31.7	29	30	34.1	30.6	29

Table 3: Carrier to noise density thresholds [5]

As an important remark, acquisition requirement only concerns aircraft operation above 1000 ft. Indeed, it is supposed that if the GNSS link is lost below this altitude, then the pilot must pursue the operation using another navigation aid, since a re-acquisition could take too much time.

C/N_0 link analysis is performed completing Table 4.

Line	Parameter	Value
1	Minimum received power of the total signal from the SV	
2	Minimum antenna gain	
3	Implementation losses	
4	Recovered satellite power C	(1)+(2)-(3)
5	Thermal noise PSD N_0	
6	Equivalent noise of aeronautical mobile satellite service (AMSS) RFI $I_{0,AMSS}$	
7	Equivalent noise of avionics radiated RFI $I_{0,case em}$	
8	Equivalent noise of RFI of other GNSS satellite transmitting within the same band $I_{0,GNSS}$	
9	Total wideband equivalent continuous RFI PSD $I_{0,aero,WB}$	(6)+(7)+(8)
10	Effect of the pulse saturation: R_I, N_{Lim}, PDC_{Lim}	
11	Efficient noise PSD $N_{0,eff}$	

12	Receive carrier to noise density ratio $C/N_{0,eff,only_aero}$	(4)-(11)
13	C/N ₀ operation threshold of the total signal	
14	Margin	(14)-(13)
	Remaining I0tolerable	

Table 4: Link budget analysis table

1.1 Minimum recovered GNSS signal power

The minimum receiver power C_{min} corresponds to the minimum received useful GNSS signal total power (data and pilot components are considered for Galileo E1 signals) on Earth. It can be recovered from [3]. The minimum antenna gain G_{min} is published in DO373 for DFMC receivers. The minimum antenna gain of DFMC receivers is also represented in Figure 3. The minimum antenna gain depends on the signal operation. Indeed, acquisition requirement imposes to obtain a position, navigation and timing (PNT) solution considering that almanacs are known. Thus, only the four highest available satellites are needed to achieve the requirement. For safety purpose, it will be considered here that the highest satellite of each core constellation is unavailable due to failure. Thus, the minimum antenna gain for acquisition scenario depends on the configuration of the GNSS constellations during the jamming period. In the zone impacted by the jammer (up to some hundreds of kilometers), the satellite elevation does not vary a lot. Therefore, a constant value G_{min} is using when completing Table 4 for acquisition scenario for all positions of the victim receiver. For tracking and demodulation cases, even though the availability of all space vehicles (SV) is not mandatory to reach accuracy requirement, an objective proposed here is to be able to track and demodulate signals coming from a SV at 5° elevation as indicated in [7]. Implementation losses L_{imp} correspond to the aggregate of losses caused by filtering, quantization and payload distortion. They are evaluated at 1.5 dB for GPS L1C/A DFMC receiver, according to [9]. Concerning Galileo E1 receiver, the computation of implementation losses is presented hereinafter.

$$L_{imp} = L_{filt} + L_{ADC} + L_{payload} \quad (11)$$

[13] indicates that the losses due to payload distortion $L_{payload}$ can be up to 0.6 dB. This component refers to non-ideal shape of the signal due to the satellite payload. RF front-end filtering and mismatch between the incoming GNSS signal (CBOC modulation) and the GNSS local replica (BOC modulation) also induce some losses, equal to

$$L_{filt} = \frac{\left(\int_{-\infty}^{+\infty} H_{RF}(f) \cdot S_{CBOC,+}(f) \cdot S_{BOC}(f) \cdot df\right)^2 + \left(\int_{-\infty}^{+\infty} H_{RF}(f) \cdot S_{CBOC,+}(f) \cdot S_{BOC}(f) \cdot df\right)^2}{2 \cdot \int_{-\infty}^{+\infty} H_{RF}(f) S_{BOC}(f) \cdot df} \quad (12)$$

BW is the double sided front-end filter bandwidth. S_{BOC} , $S_{CBOC,+}$, $S_{CBOC,-}$ are respectively the normalized power spectral density of a BOC(1,1), CBOC(6,1,1/11,+) and CBOC(6,1,1/11,-) modulated signal. H_{RF} is the transfer function of the RF front-end filter. With a 12 MHz double sided filter, L_{filt} is evaluated at 0.36 dB. Finally, quantization losses using a 1.5 bit analog to digital converter (ADC) induces a 0.916 dB loss [10]. The total implementation losses for DFMC Galileo receiver is thus 1.9 dB. Once implementation losses are evaluated, the recovered signal power can be computed from the received power at the antenna input, the antenna gain and implementation losses. Recovered signal power designates the power of the useful signal at the antenna port as if all subsequent elements (RFFE, AGC/ADC, correlator) are ideal and do not bring any power losses. Equivalently, the recovered signal power is also the GNSS signal power at the correlator input. It depends on the signal sig (GPS L1C/A, Galileo E1OS, SBAS L1) as well as the GNSS receiver signal processing operation (acquisition, tracking, demodulation) op through the influence of the receiver antenna gain (different lowest elevation angles are considered for each operation). $C(sig, op)$ is mathematically expressed as:

$$C(sig, op) = C_{min}(sig) \cdot G_{min}(sig, op) \cdot L_{imp}(sig) \quad (13)$$

1.2 Efficient noise in presence of non-aeronautical RFI

Efficient noise power density level, $N_{0,eff,aero_only}$, considering all aeronautical RFI sources is derived with the following formula:

$$N_{0,eff,aero_only} = \frac{N_0}{1 - PDC} \cdot \left(1 + \frac{I_{0,aero}}{N_0} + R_I + N_{lim}^2 \cdot \frac{PDC}{1 - PDC}\right) \quad (14)$$

N_0 is the thermal noise power spectral density level. The maximum value for L1 receiver is -201.5 dBW/Hz, according to [7]. PDC is the pulse duty cycle and corresponds to the amount of time that the LNA is saturated and does not operate in a linear way. Even though the L1 band is in theory not impacted by high power pulsed RFI, a 1% value is proposed for PDC [7]. $I_{0,aero}$ is the aggregate of all aeronautical RFI equivalent noise power density level (previously defined AMSS, case emission and inter/intra system). R_l is the ratio of below saturation average pulse power density to N_0 . It quantifies the effect of a pulsed RFI which is not powerful enough to reach the saturating point of the LNA (low noise amplifier). For the L1 band, R_l is supposed to be null. N_{lim} is the ratio of analog to digital saturation level to $1 \cdot \sigma$ noise voltage established by AGC (equal to 1.5 for a 1.5 bit ADC).

As highlighted earlier, the aeronautical RFI equivalent noise depends on the position on Earth of the victim receiver. However, in the zone impacted by the jammer (up to some hundreds of kilometers), aeronautical RFI environment can be considered uniform. Therefore, a unique value is used when completing Table 4 and this value does not depend on the GNSS receiver operation (acquisition, tracking, demodulation) nor on the position of the victim receiver in the zone impacted by the jammer.

1.3 Link budget margin

Then, the minimum carrier to efficient noise ratio is computed. This $C/N_{0,eff}$ ratio is compared to the C/N_0 threshold for the considered operation to deduce the margin. The C/N_0 margin is defined by

$$Margin(sig, op) = \frac{C(sig, op)/N_{0,eff}}{C/N_{0Th}(sig, op)} \quad (15)$$

1.4 Maximum tolerable non-aeronautical RFI

Eventually, the maximum equivalent noise from non-aeronautical sources that a receiver can tolerate can be derived. It is given by:

$$I_{0,non\ aero,max}(sig, op) = N_{0,eff} \cdot (Margin(sig, op) - 1) \cdot (1 - BDC) \quad (16)$$

2. Non-aeronautical RFI level:

Once the non-aeronautical RFI level that can be tolerated by the receiver is known, the second step of the new proposed method consists in computing the equivalent noise caused by all non-aeronautical sources impacting the GNSS band. Non-aeronautical RFI sources have been detailed earlier in this article. The aggregate non-aeronautical RFI level faced by a victim receiver depends on its position (x, y) in the local reference frame centered at the jammer and its altitude h .

$$I_{0,non\ aero}(x, y, h) = M \cdot I_{0,on\ board} + M \cdot I_{0,terr}(x, y, h) + I_{0,jam}(x, y, h) \quad (17)$$

M is a margin added on on-board PEDs and terrestrial emitters contribution to cover uncertainties on path losses and transmitted power. Usually, a 6 dB margin is considered. During military jamming exercises, a well calibrated jammer is used. Therefore, no margin is added on the jammer contribution. If jammer power stability is uncertain, then it is advised to add a margin on $I_{0,jam}(x, y, h)$ to cover power fluctuation.

3. Protection zone determination:

The third and last step of the new proposed method consists in deriving the protection zone. The protection zone is derived as follows. First, for each signal sig , each GNSS receiver fundamental operation op , a protection radius $r_{sig,op}(h)$ at the altitude h is computed by finding all positions of the victim receiver (x, y) in the local reference frame centered at the jammer position at altitude h for which the minimum requirement on signal sig and fundamental operation op is not fulfilled. $r_{sig,op}(h)$ is mathematically expressed by

$$r_{sig,op}(h) = \max_{x,y} \{ \sqrt{x^2 + y^2} \mid I_{0,non\ aero}(x, y, h) \geq I_{0,non\ aero,max}(sig, op) \} \quad (18)$$

Second, the protection zone that is derived with the new methodology has a cylinder shape whose height is the maximum aircraft flight level and radius is the worst protection radius $r_{sig,op}(h)$ among all signals, receiver operations and altitudes: $\max_{sig,op,h} r_{sig,op}(h)$.

COMPARISON OF PROTECTION ZONES ON AN ILLUSTRATIVE JAMMING SCENARIO

Previous section detailed how a protection zone is derived using the new proposed method. In this section, the protection zone derived with the new method is compared to the protection zone derived using the traditional approach based on RFI mask. A fictive jamming exercise is assumed to take place in France, at the position 46.1°N,0.18°E. The date of jamming is 2021, April 17th and is assumed to last 24h. The state jammer is located on the ground and transmits a signal with rectangular shape power spectral density. The jamming signal characteristics are presented in Table 5.

Power (W)	Antenna gain (dB)	Bandwidth (MHz)	Central frequency
12	5 (antenna supposed to be omnidirectional)	50	L1

Table 5: Jammer settings

A protection zone for DFMC (dual frequency and multi constellation) receivers is derived.

Now, let us compute the protection zone using the new proposed method. Link budget analysis for Galileo E1 OS signal and for GPS L1 C/A / SBAS L1 signals at the position of the jammer are presented in Table 6 and Table 7. In order to determine the minimum antenna gain for acquisition scenarios, GNSS constellations have been run over the period of jamming. The minimum elevation over the jamming period of the second highest satellite and the fifth highest satellite are respectively:

- For Galileo: 34.1° (antenna gain: 0.592 dB) and 9.2° (antenna gain: -3.230 dB).
- For GPS: 46.8° (antenna gain: 0.874 dB) and 16.5° (antenna gain: -1.296 dB).

Moreover, the inter/intra system RFI at the position of the jammer is -200.07 dBW/Hz on a Galileo BOC(1,1) receiver and -200.24 dBW/MHz on a GPS L1C/A and SBAS receivers (respectively taken from Figure 4 and Figure 5).

#	Parameter (Units)	Acq. s/v 1 Value	Acq. s/v 4 Value	Gal r-Trk Value
1	Min. SV Earth Surface Power (dBW)	-157,90	-157,90	-157,90
2	Receive Antenna Gain (dBic)	0,592	-3,230	-4,500
3	Implementation Loss (dB)	1,90	1,90	1,90
4	RFI-free Post-Corr Carrier Pwr (dBW)	-159,21	-163,03	-164,30
5	$I_{0,AERO}/N_0$ (ratio)	1,605457	1,605457	1,605457
8	$N_{0,EFF}/N_0$ (ratio)	2,654732	2,654732	2,654732
9	$N_{0,EFF}$ dB(W/Hz)	-197,260	-197,260	-197,260
10	Effective Carrier/(Noise+RFI) ratio (dB-Hz)	38,052	34,230	32,960
11	Min. CNIR (dB-Hz)	34,10	30,60	29,00
12	Link Margin (dB)	3,952	3,630	3,960
13	Remaining I0tolerable	-195,589	-196,142	-195,575

Table 6: Galileo E1 C/N0 link budget

#	Parameter (Units)	Acq. s/v 1 Value	Acq. s/v 4 Value	GPS r-Trk Value	SBAS Demod value
1	Min. SV Earth Surface Power (dBW)	-158,50	-158,50	-158,50	-158,5
2	Receive Antenna Gain (dBic)	0,874	-1,296	-4,500	0,65
3	Implementation Loss (dB)	1,50	1,50	1,50	1,50
4	RFI-free Post-Corr Carrier Pwr (dBW)	-159,13	-161,30	-164,50	-159,35
5	$I_{0,AERO}/N_0$ (ratio)	1,551497	1,551497	1,551497	1,551497
8	$N_{0,EFF}/N_0$ (ratio)	2,600227	2,600227	2,600227	2,6002654
9	$N_{0,EFF}$ dB(W/Hz)	-197,350	-197,350	-197,350	-197,34989
10	Effective Carrier/(Noise+RFI) ratio (dB-Hz)	38,224	36,054	32,850	38,00
11	Min. CNIR (dB-Hz)	32,40	31,70	29,00	30,00
12	Link Margin (dB)	5,824	4,354	3,850	8,00
13	Remaining I0tolerable	-192,887	-195,025	-195,851	-190,14307

Table 7: GPS L1C/A and SBAS L1 C/N0 link budgets

Analyzing Table 6 and Table 7, it can be observed that the most constraining scenario is the acquisition of the fourth highest Galileo satellite. This is mainly due to the fact that Galileo constellation at the jamming date has only 22 active satellites which implies that the Galileo SV with highest elevation angle for acquisition has lower elevation angle than the GPS L1C/A SV with highest elevation angle. Remember that acquisition requirements only concern aircraft operation above 1000 ft. For aircraft operation below this altitude, the most constraining case is the GPS L1C/A tracking of a signal coming from a 5° elevation angle SV. In this case, the non-aeronautical equivalent noise must be lower than -195.85 dBW/Hz.

During the second step of the new methodology, the non-aeronautical RFI equivalent noise is computed around the jammer. Figure 8 shows the non-aeronautical equivalent noise at a 500 m altitude around the jammer position, $I_{0,non\ aero}(x, y, h = 500)$. As discussed before, a 6 dB margin is added to the noise level induced by terrestrial emitters and on-board PEDs. No margin is added on the jammer noise level. Indeed, the power transmitted by the jammer during state jamming operations is well calibrated and monitored. From equation (2), the spectral separation coefficient between the jamming signal used in our illustrative case and a BPSK GPS L1C/A local replica with a 12 MHz RFFE double-sided filter bandwidth receiver is equal to -77.06 dB. For a BOC(1,1) Galileo E1 receiver, considering a 12 MHz double sided RFFE, SSC_j is equal to -77.21 dB.

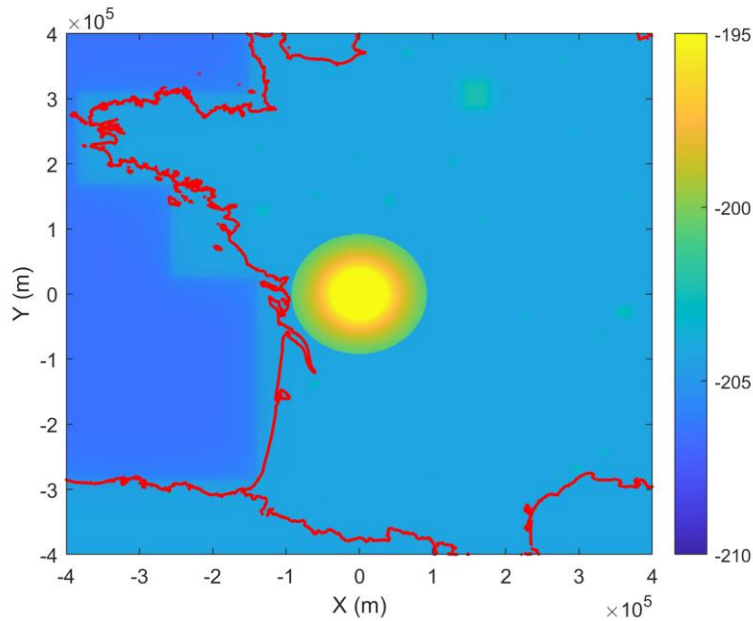


Figure 8: Equivalent noise (dBW/Hz) caused by non-aeronautical sources at 500 m altitude

Figure 8 highlights that the jammer is the main contributor on the non-aeronautical equivalent noise, but terrestrial and on-board transmitters cannot be neglected. In order to determine the protection zone, the protection radius is computed at different altitudes, for all signals and operations. Figure 9 illustrates the evolutions of $r_{sig,op}(h)$ with the altitude.

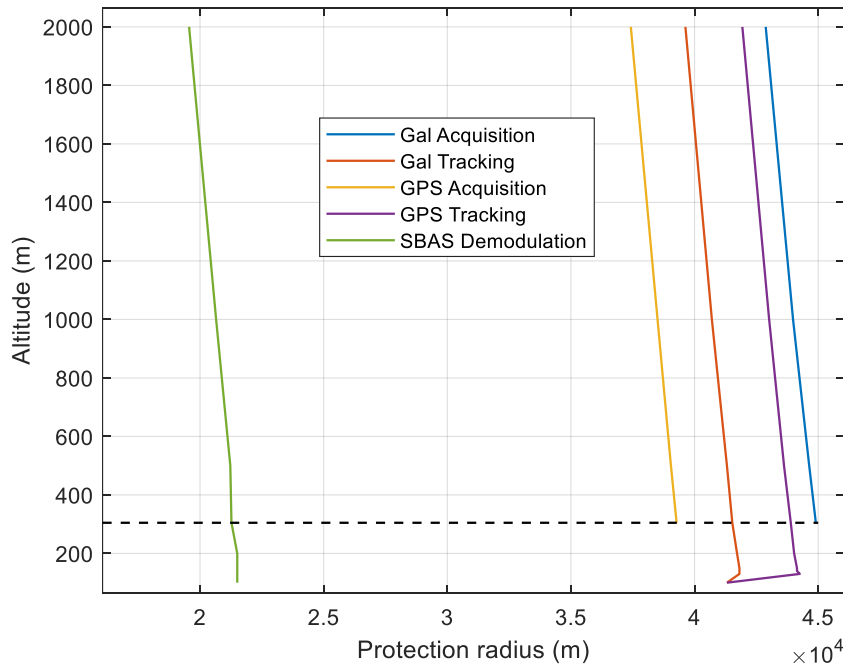


Figure 9: Evolution of the protection radius with the altitude for all signals and operations

Several key points must be analyzed in Figure 9. First, for altitudes below 120 m, the non-aeronautical equivalent noise is higher than the maximum non-aeronautical equivalent noise tolerable by the receiver at all points where the jammer is visible from the victim aircraft. Thus, for altitudes below 120m, the tracking protection radius is equal to the radio line of sight range. Then, for

altitudes between 120 m and 1000 ft (304.8 m), the tracking protection radius slowly decreases. This is mainly due to an increase of propagation path losses along the increase of the altitude. For altitude above 1000 ft, the limiting processing operation is the acquisition of the fourth Galileo E1 satellite whereas the limiting signal processing operation was the GPS L1C/A tracking for altitudes below 1000 ft. The maximum protection radius among all altitudes is 44.9 km (reached at a 1000 ft altitude by the fourth Galileo SV acquisition). Thus, a protection area that can be proposed in order to guarantee the operation of GNSS receivers is a cylinder with 45 km radius, centered on the position of the jammer.

The protection radius using the traditional RFI mask method is then determined using equation (1). For a 50 MHz RFI, C_{max} is equal to -96.5 dBm according to [8]. Note that on-board PEDs and terrestrial emitters are not taken into account in this method. Table 8 recaps the protection radius computed from the two methods.

	RFI mask method	New method
Protection radius (km)	45	99

Table 8: Comparison of the protection radius obtained by the two methods

The protection radius computed from the RFI mask would be 99 km. Therefore, the new method proposal allows to reduce by more than 50% the protection zone in our illustrative jamming scenario.

CONCLUSION AND WAY FORWARD

This paper provides a methodology to derive a protection radius during state jamming operations. This work is motivated by a request of the French ANSP (Air Navigation Service Provider), since the observed impact radius of the jammer during state jamming operation was much lower than the radius predicted from the RFI mask.

A protection zone is a volume determined by the regulator and communicated to pilots on which GNSS minimum requirements may not be met. The fundamental idea of the method proposed in this article to derive the protection area consists in a fine characterization of the RFI situation faced by the victim receiver. The protection zone limit will be such that the aggregate RFI level is equal to the maximum RFI level tolerated by the receiver. The three main methods are recalled hereinafter. First, a fine C/N_0 link budget allows to determine how much non-aeronautical RFI can be tolerated by the receiver. Second, the aggregate non-aeronautical RFI faced by the receiver is computed. Third, protection area is derived. The protection area includes all position for which the non-aeronautical RFI equivalent noise received by the victim aircraft exceed the non-aeronautical level tolerated to keep minimum operational requirements satisfied. In the illustrative situation presented above, the protection area is reduced by more than 50% in comparison to the protected zone derived from the RFI mask.

As a way forward, this new methodology must be adapted in case of high jamming power, taking into account tropospheric reflection which are not considered in this paper. For safety reason and before to be adopted, this method should be validated during a real jamming scenario, comparing the zone impacted in reality with the protection area derived with the new methodology.

REFERENCES

[1] Radio Technical Commission for Aeronautics, “DO 229E - Minimum Operational Performance Standards (MOPS) for GPS/WAAS Airborne Equipment,” DO 229E, Dec. 2016.

[2] Radio Technical Commission for Aeronautics, “DO 292 - Assessment of Radio Frequency Interference Relevant to the GNSS L5/E5A Frequency Band,” Jul. 2004.

[3] International Civil Aviation Organization (ICAO), “International standards and recommended practices for aeronautical telecommunications,” *Annex 10 to the convention of international civil aviation*, 2020.

[4] M. Johnson and R. Erlandson, “GNSS Receiver Interference: Susceptibility and Civil Aviation Impact,” Palm Springs, 1995, pp. 781–791.

[5] RTCA, “DO 235C - Assessment of Radio Frequency Interference Relevant to the GNSS L1 Frequency Band,” 2021.

[6] A. Garcia-Pena, C. Macabiau, O. Julien, M. Mabilieu, and P. Durel, “Impact of DME/TACAN on GNSS L5/E5a Receiver,” San Diego, California, Feb. 2020, pp. 207–221. doi: 10.33012/2020.17207.

[7] Radio Technical Commission for Aeronautics, “DO 235B - Assessment of Radio Frequency Interference Relevant to the GNSS L1 Frequency Band,” Mar. 2008.

- [8] Radio Technical Commission for Aeronautics, “DO-160G - Environmental Conditions and Test Procedures for Airborne Equipment,” 2010.
- [9] Radio Technical Commission for Aeronautics, “DO 235C - Assessment of Radio Frequency Interference Relevant to the GNSS L1 Frequency Band,” 2022.
- [10] J. J. Ely, T. X. Nguyen, S. V. Koppen, and J. H. Beggs, “Wireless Phone Threat Assessment and New Wireless Technology Concerns for Aircraft Navigation Radios.”
- [11] Radio Technical Commission for Aeronautics, “DO-373 - MOPS for GNSS Airborne Active Antenna Equipment for the L1/E1 and L5/E5a Frequency Bands,” 2018.
- [12] C. J. Hegarty, “Analytical Model for GNSS Receiver Implementation Losses,” *Navigation*, vol. 58, no. 1, pp. 29–44, Mar. 2011, doi: 10.1002/j.2161-4296.2011.tb01790.x.
- [13] European GNSS Agency, “European GNSS (Galileo) Open Service Signal-in-Space Interface Control Document,” 2021.
- [14] GPS, “Interface Specification GPS 200L,” 2020.
- [15] T. X. Nguyen, S. V. Koppen, J. J. Ely, R. A. Williams, L. J. Smith, and M. T. P. Salud, “Portable wireless device threat assessment for aircraft navigation radios,” in *2004 International Symposium on Electromagnetic Compatibility (IEEE Cat. No.04CH37559)*, Silicon Valley, CA, USA, 2004, pp. 809–814. doi: 10.1109/ISEMC.2004.1349926.